JOURNAL OF NATURAL PRODUCTS

Article

Cite This: J. Nat. Prod. 2019, 82, 66−73

pubs.acs.org/jnp

C-Phycocyanin from *Spirulina* Inhibits α-Synuclein and Amyloid-β Fibril Formation but Not Amorphous Aggregation

Yanqin Liu,[†,‡,§] Blagojce Jovcevski,[‡,§] and Tara L. Pukala*[,‡]

[†]The School of Technology, Hebei Agricultural University, Cangzhou, Hebei 061100, People's Republic of China

[‡]The School of Physical Sciences, The University of Adelaide, Adelaide, South Australia 5005, Australia

Supporting Information

ABSTRACT: Proteinopathies including cataracts and neurodegenerative diseases, such as Alzheimer's and Parkinson's disease, are characterized by a series of aberrant protein folding events, resulting in amorphous aggregate or amyloid fibril formation. In the latter case, research has heavily focused on the development of small-molecule inhibitors with limited success during clinical trials. However, very few studies have focused on utilizing exogenous proteins as potential aggregation inhibitors. C-Phycocyanin, derived from *Spirulina* sp., has been known to exert anti-inflammatory properties; however, the ability of C-phycocyanin to inhibit protein aggregation has yet to be investigated. We have demonstrated that C-phycocyanin is an effective inhibitor of A53Tα-synuclein at extremely low substoichiometric ratios (200-fold excess of α-synuclein) and Aβ40/42 fibril formation. However, C-phycocyanin is relatively ineffective in inhibiting the reduction-induced amorphous aggregation of ADH and heat-induced aggregation of catalase. In addition, 2D NMR, ion mobility-mass spectrometry, and analytical-SEC demonstrate that the interaction between C-phycocyanin and α-synuclein is through nonstable interactions, indicating that transient interactions are likely to be responsible for preventing fibril formation. Overall, this work highlights how biomolecules from natural sources could be used to aid in the development of therapeutics to combat protein misfolding diseases.

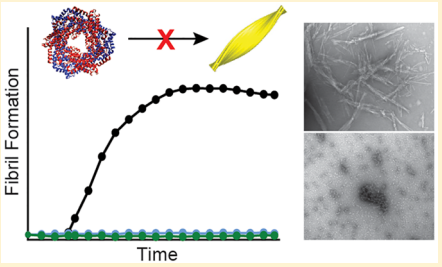

A large number of diseases with significantly different pathologies can be attributed to defects in the protein quality control network, resulting in protein misfolding, and are typically characterized by the eventual formation of either amorphous aggregates or amyloid fibrils. Fibril formation is a hallmark of multiple neurodegenerative diseases, including Parkinson's and Alzheimer's disease, which are mediated by the misfolding and aggregation of proteins such as α-synuclein (αS) and amyloid-β (Aβ), respectively.[1] Under conditions of cellular stress (e.g., disease, oxidative stress, changes in pH), these proteins are known to self-associate into well-defined supramolecular, fibrillar structures with high cross β-sheet content.[2] Conversely, the deposition of unstructured amorphous aggregates gives rise to diseases such as cataracts, whereby the destabilization of β- and γ-crystallins through mutation and chemical damage leads to the formation of amorphous aggregates, resulting in lens opacification and blindness.[3] Therefore, there has been increased demand to identify molecules capable of preventing and/or modulating the destabilization of aggregation-prone proteins, providing critical information for the development of effective therapeutics against disease.

Previous studies have identified a range of small molecules (e.g., polyphenols and small peptides) that appear to impede fibril formation *in vitro*;[4−7] however the mechanism(s) by which this occurs remains largely unclear, and to date no effective therapeutic has been developed for widespread treatment. Consequently, exploring novel approaches to combat protein misfolding and aggregation is crucial for the prevention and treatment of these diseases. An alternative therapeutic approach to the treatment of protein misfolding diseases could involve the use of natural, chemical, or pharmacological chaperones. Molecular chaperone proteins are responsible for facilitating folding of other proteins toward a native (functional) structure.[8−10] In the cell, molecular chaperones (e.g., chaperonins) interact with the exposed hydrophobic surfaces of a non-native protein, which modulate folding kinetics and enhance folding efficiency.[11] In addition, other molecular chaperones (e.g., small heat-shock proteins; sHsps) also stabilize non-native structures to prevent the formation of misfolded and/or aggregated species.[8,12] Typically, molecular chaperones are multi-subunit assemblies and, in the case of chaperonins, form a stacked double-ring structure, which is thermally stable, necessary for managing protein folding in response to cellular stress.[13,14]

C-Phycocyanin (C-PC) is a major phycobiliprotein derived from blue-green algae (*Spirulina* sp.) and is widely used in food supplements due to its antioxidative, anti-inflammatory, hepatoprotective, and neuroprotective properties both *in vitro* and *in vivo*.[15−17] Structurally, C-PC forms a hetero-oligomer composed of α- (18.2 kDa) and β- (19.3 kDa) subunits, which assemble into a ring-shaped quaternary conformation (Figure S1). C-PC is also a dynamic protein, occupying a range of

Received: July 26, 2018
Published: January 8, 2019

DOI: 10.1021/acs.jnatprod.8b00610
J. Nat. Prod. 2019, 82, 66−73

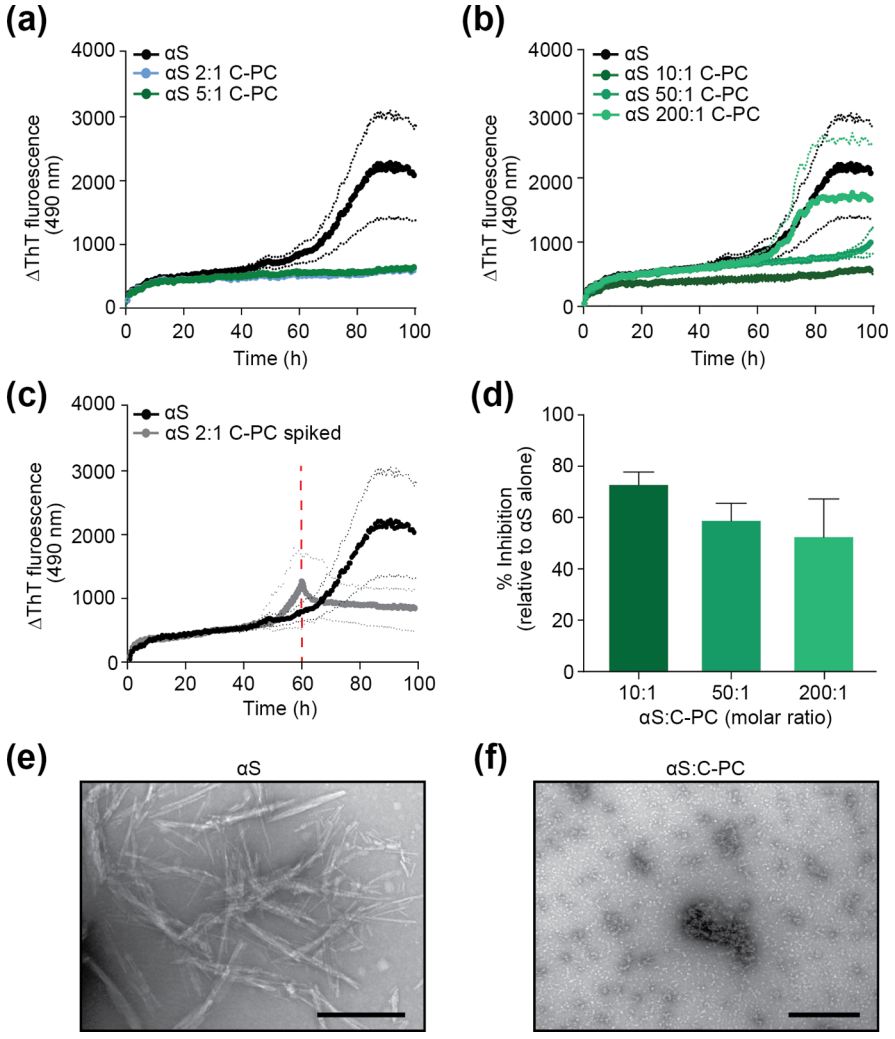

Figure 1. C-PC significantly inhibits A53TαS fibril formation at substoichiometric ratios. (a) Fluorescence-detected ThT aggregation assay of αS (10 μM; black) in the presence of C-PC at 2:1 (green) and 5:1 (blue) molar ratios (αS:C-PC). Assays were performed in 500 mM ammonium acetate buffer (pH 7.4) at 37 °C (mean ± SEM, n = 3). (b,d) Concentration-dependent inhibition of αS (10 μM) fibril formation as determined by ThT aggregation assays (mean ± SEM, n = 3). (c) ThT aggregation assay of αS (10 μM) spiked after 60 h (red dashed line) with C-PC (5 μM; grey) following incubation, halting further fibril elongation. (e, f) TEM analysis of αS fibrils (10 μM) following 100 h of incubation in the absence (e) and presence (f) of C-PC (2 μM). Scale bars represent 500 nm.

oligomeric states (predominantly dimeric or dodecameric), which are modulated by pH, ionic strength, temperature, and concentration.[18,19] A previous study has shown selenium-containing phycocyanin can inhibit islet amyloid polypeptide fibril formation and prevent β-cell apoptosis.[20] Overall, C-PC shares some structural and functional characteristics with molecular chaperones that prevent protein misfolding and aggregation.

In this study we sought to investigate the inhibitory properties of C-PC in arresting the aggregation of disease-associated proteins, namely, αS (disease mutant A53T) and Aβ (Aβ 1−40 and Aβ 1−42). Furthermore, we also examined conformational changes and interaction dynamics of aggregation-prone proteins, in the presence and absence of C-PC, by means of NMR spectroscopy, size exclusion chromatography and ion mobility−mass spectrometry (IM-MS).

RESULTS AND DISCUSSION

C-Phycocyanin Inhibits Primary Nucleation and Fibrillation of αS. The ability of C-PC to inhibit A53TαS (αS herein) amyloid formation was examined using thioflavin-T (ThT) fluorescence assays, which measure the changes in fluorescence of the ThT dye upon binding to cross β-sheet rich structures formed during fibrillation.[21] In the absence of αS, C-PC does not show any evidence of self-fibrillation, with no increase in ThT fluorescence observed (Figure 1a). In contrast, in the absence of C-PC, ThT fluorescence increased with αS incubation time, consistent with fibril formation over a period of approximately 80 h (Figure 1a). The presence of C-PC at a 2:1 (αS:C-PC) molar ratio was able to negate any increase in ThT fluorescence, indicating significant inhibition of fibril formation (Figure 1a). Furthermore, the chaperone-like activity of C-PC is concentration-dependent when tested at a range of αS:C-PC molar ratios (10:1, 50:1, and 200:1), exhibiting ∼50% inhibition at extremely low molar ratios (200:1) (Figure 1b and 1d).

The ability of C-PC to reverse partially aggregated αS was also examined by changes in ThT fluorescence. The addition of C-PC to A53TαS during the fibril elongation phase (after 60 h) at a 2:1 molar ratio halted further increases in ThT

DOI: 10.1021/acs.jnatprod.8b00610
J. Nat. Prod. 2019, 82, 66−73

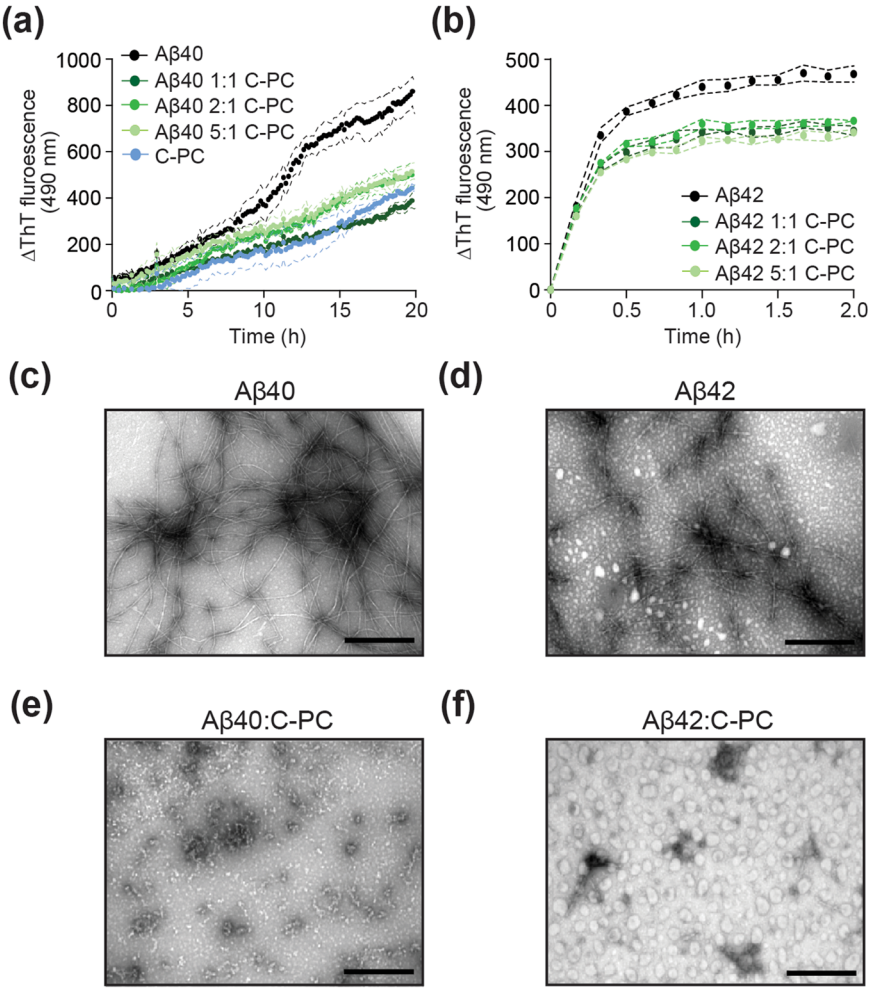

Figure 2. C-PC inhibits Aβ40/42 fibril formation at substoichiometric ratios. Fluorescence-detected ThT aggregation assay of Aβ40 (a) and Aβ42 (b) (both 10 μM) in the absence (black) and presence (green) of C-PC at a 5:1 molar ratio (Aβ:C-PC). Assays were performed in 500 mM ammonium acetate buffer (pH 7.4) at 37 °C (mean ± SEM, n = 3). (c–f) TEM analysis of Aβ40 (10 μM) following 25 h of incubation and Aβ42 (10 μM) following 2 h of incubation, in the absence (c, d) and presence (e, f) of C-PC (2 μM). Scale bars represent 500 nm.

fluorescence, appearing to prevent further fibril elongation/formation, but also resulted in a slight decrease in ThT fluorescence, indicative of some fibril disassembly (Figure 1c). This suggests that C-PC interferes with both nucleation and elongation of αS fibrils. To confirm the prevention of fibril formation, TEM was conducted to observe the morphology of αS after incubation in the absence and presence of C-PC. An abundance of long, mature fibrils was detected for αS alone after 100 h of incubation (Figure 1e). In contrast, αS incubated with C-PC did not form mature fibrils, but rather large amorphous aggregates were observed (Figure 1f).

C-PC Has Broad Antiamyloidogenic Activity but Does Not Prevent Amorphous Aggregation. To determine whether the ability of C-PC to inhibit fibril formation was specific to αS, analogous ThT and TEM studies were also performed with other fibril-forming proteins, namely, Aβ40 and Aβ42. As observed for A53TαS, the characteristic increase in ThT fluorescence occurring during fibril formation for both Aβ40/42 was prevented by the presence of substoichiometric molar ratios (5:1) of C-PC (Figure 2a,b). However, the degree of inhibition was less than that observed for αS at the equivalent molar ratios tested. In addition, TEM images also show the difference in the morphology of Aβ40/42 fibrils, where long, mature fibrils were abundant in the absence of C-PC (Figure 2c,d). In comparison, Aβ40/42 in the presence of C-PC substantially reduced the abundance of fibrils, forming small fibril clusters (Figure 2e,f). In all, C-PC appears to be also effective in inhibiting Aβ40/42 fibrillation, but not to the same extent when compared to αS fibril inhibition.

The ability of C-PC to inhibit the amorphous aggregation of ADH and catalase was also investigated by measuring the changes in absorbance at 340 nm, indicative of light scattering caused by amorphous aggregate formation. In the absence of C-PC, ADH and catalase begin to form amorphous aggregates after 20 min, with absorbance changes beginning to plateau after 90 min (Figure 3). In the presence of C-PC, there was an observable decrease in light scattering of ADH (Figure 3a) at a 2:1 molar ratio (ADH:C-PC). Conversely, there was an increase in light scattering of catalase in the presence of C-PC (2:1) (catalase:C-PC) relative to catalase alone (Figure 3b). Given that the incubation of C-PC alone resulted in a slight increase in absorbance under amorphous assay conditions (42 °C for ADH and 55 °C for catalase), the data demonstrate that the inhibitory action of C-PC is dependent on both the morphology of aggregation-prone protein and assay conditions,

DOI: 10.1021/acs.jnatprod.8b00610
J. Nat. Prod. 2019, 82, 66–73

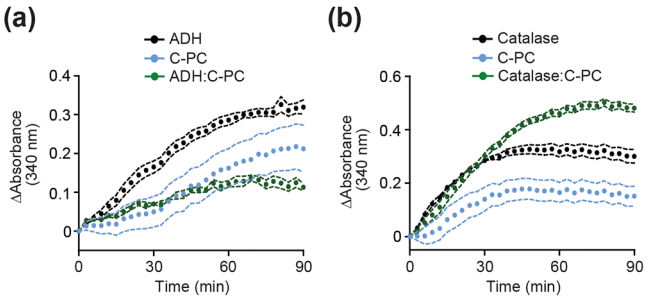

Figure 3. C-PC is ineffective at inhibiting amorphous aggregation of ADH and catalase. The ability of C-PC to inhibit the heat-induced amorphous aggregation of ADH (a) and catalase (b) was measured by the change in light scattering at 340 nm. ADH or catalase (both 5 μM) was incubated in the absence (black) or presence of C-PC (2.5 μM) (green). C-PC in the absence of ADH and catalase shows no change in light scattering under these conditions (blue). Assays were performed in 50 mM phosphate buffer (pH 7.4) at 40 °C (mean ± SEM, n = 3).

with specificity toward proteins that form amyloid fibrils at physiologically relevant conditions.

The Interaction between C-PC and A53TαS Is Not Stable. To investigate the interactions between monomeric A53TαS and C-PC, the latter was titrated into uniformly ^{15}N-labeled αS, and ^{1}H−^{15}N HSQC experiments were performed to monitor changes in amide chemical shifts, using previously described resonance assignments[22] (Figure 4). In the presence of C-PC, few significant chemical shift changes were observed, with the largest perturbation at H50, likely a result of sensitivity to small changes in pH.[22,23] In addition, a small, uniform reduction in the signal-to-noise ratio was observed for αS in the presence of C-PC (Figure 4, right panel).[24] Overall, the lack of selective chemical shift changes or broadening of specific αS resonances suggests that the binding of C-PC may not involve specific residues on the αS monomers.

The interaction between αS and C-PC was further characterized by native mass spectrometry (MS) (Figure 5a). Under instrument conditions suited to maintaining non-covalent interactions in the gas phase,[25,26] no distinct complex between A53TαS and C-PC was observed following co-incubation for 20 h (Figure 5a). Instead, the oligomeric state of αS was observed primarily as monomer and dimers, with the monomer displaying an increased abundance of lower charge states (monomer^{7+} being the most abundant) compared to those typically observed for αS (Figure 5a). The oligomeric state of C-PC is predominantly dimeric; however, a small population of dodecamer could also be observed under these instrument conditions (Figure 5a). To further confirm the nature of the interactions between αS and C-PC, the proteins were incubated and subject to analytical size-exclusion chromatography (SEC) to identify whether C-PC forms a stable complex with αS observable in solution. Our data show that in the presence of C-PC, αS does not form a large high molecular complex (Figure 5b). The data further demonstrate that C-PC does not form a stable complex with αS to prevent fibrillation, which indicates that the interaction between αS and C-PC is weak and/or transient.

C-PC Retains the Native Structure of A53TαS. The ability of C-PC to induce conformational changes in αS monomers during aggregation was examined by IM-MS. IM-MS is capable of separating ions based on the rate at which they migrate through a region of buffer gas under the influence of an external electric field. The mobility of an ion is dependent on the collision cross section (CCS), which in turn is related to structural features (i.e., conformation) and can be determined by measurement of the ion population drift time or arrival time distribution (ATD).[27] The ATD of αS monomers was measured across a range of charge states (6+ to 14+) at 0 and 20 h of incubation, and the CCS of these ions was calculated by calibration against protein standards of known CCS.[28] To determine how C-PC affects the conformation of αS monomers, the monomer^{11+} of αS was chosen for relative

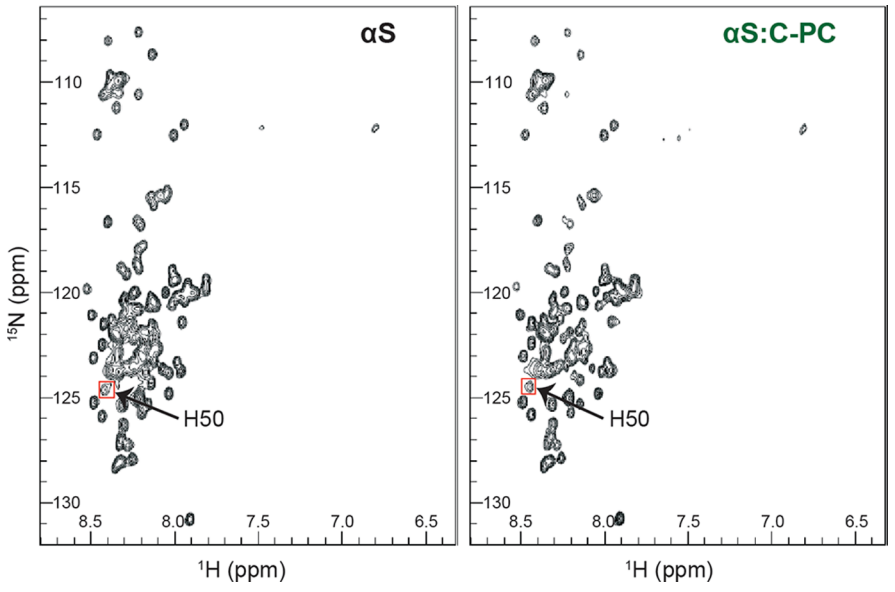

Figure 4. Stable and high-affinity interactions between A53TαS and C-PC are not observed on the NMR time scale. ^{1}H−^{15}N correlation (HSQC) spectra of αS (150 μM) in the absence (left pane) and presence (right panel) of C-PC (7.5 μM). The chemical shift observed for H50 is likely a consequence of localized pH changes and not of interaction with C-PC. NMR experiments were performed in 10 mM Na_2HPO_4 and 100 mM NaCl (pH 7.4).

DOI: 10.1021/acs.jnatprod.8b00610
J. Nat. Prod. 2019, 82, 66−73

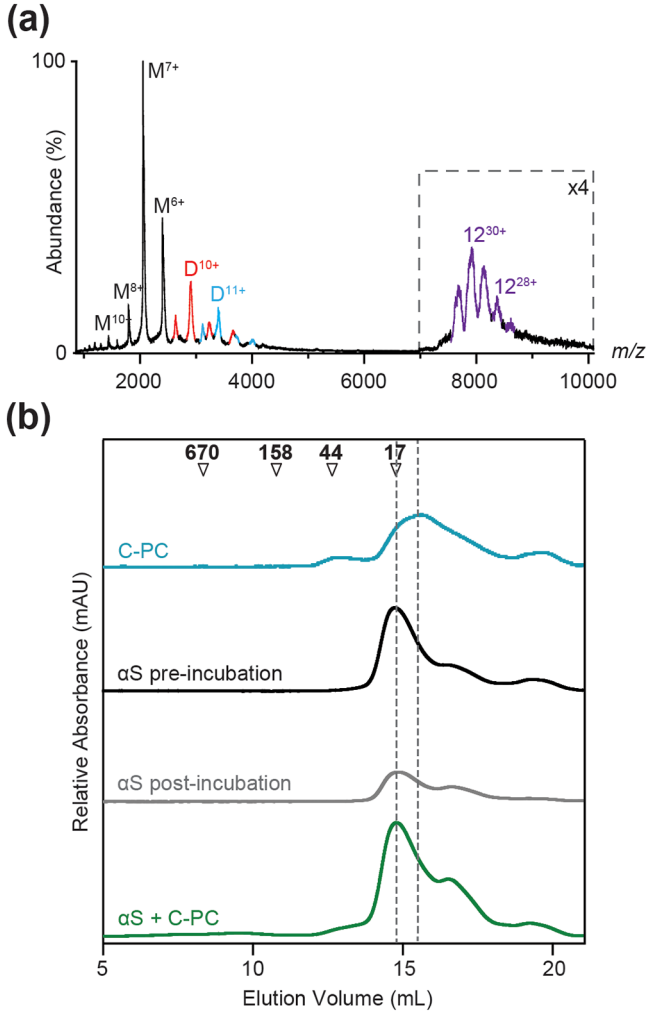

Figure 5. Stable interactions between A53TαS and C-PC are not observed by native MS and analytical-SEC. (a) Native MS spectrum of αS (10 μM) following incubation with C-PC (2 μM) at 40 °C for 20 h. No complex between αS and C-PC was observed as the spectrum was predominantly populated with A53TαS monomer (M; black) and dimer (D; red), while C-PC was predominantly a mixture of dimers (D; blue) and dodecamer (12; purple). Spectra zoomed in from 7000−10 000 m/z (gray box) and charge state of each oligomer denoted as a superscript. (b) Analytical-SEC of αS pre- (black) and postincubation (gray) in the absence and presence of C-PC (green) at a 2:1 molar ratio (αS:C-PC). The elution volumes of monomeric αS and C-PC are indicated (gray dashed line). Elution volumes of molecular weight standards (kDa) are indicated above the chromatogram.

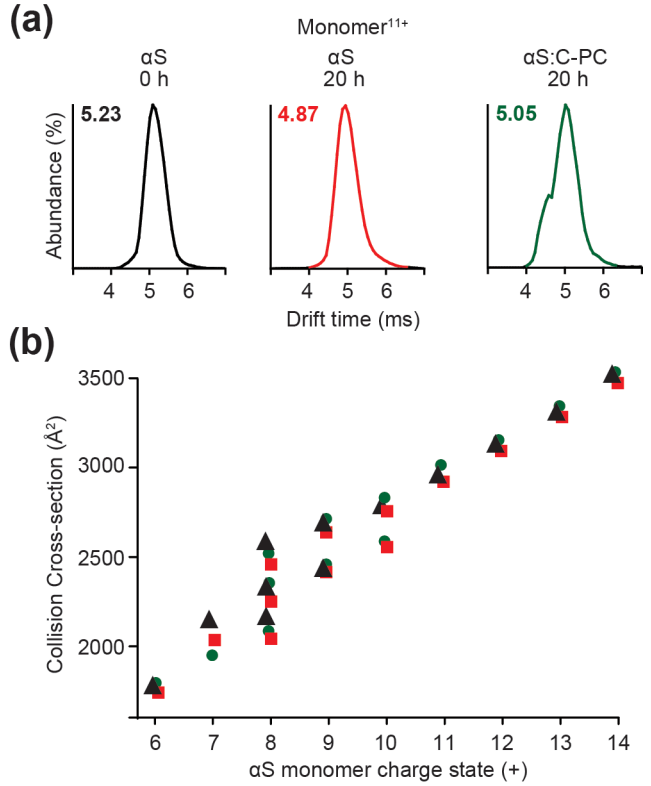

Figure 6. Arrival time distribution analysis of A53TαS monomer following incubation with C-PC. Arrival time distribution (ATD) and collision cross-section areas for αS monomer^{11+} (10 μM) following 0 h (black) (a) and 20 h of incubation at 37 °C in the absence (red) (b) and presence (green) (c) of C-PC (2 μM) (wave height: 8 V). (d) Plot of collision cross-section area as a function of charge of αS monomer following 0 h (black triangles) and 20 h of incubation at 37 °C in the absence (red squares) and presence (green circles) of C-PC (2 μM).

comparison (Figure 6a). The incubation (20 h) of αS in the absence of C-PC resulted in a decrease in the ATD (from 5.23 ms to 4.87 ms) of the monomer compared to αS prior to incubation (Figure 6a). In comparison, when αS was incubated in the presence of C-PC, there is a notable reduction in the extent of ATD decrease for the αS monomer (to just 5.05 ms) (Figure 6a).

Calculated CCSs for monomeric αS correlate with previous IM-MS studies, which observe CCS in the range 1400−2800 Å^2[29,30] and molecular size measurements from experimental small-angle X-ray scattering data (with a radius of gyration of approximately 40 Å).[31] In addition, the decrease in ATD (and in turn CCS) in the presence of C-PC was consistent across the charge states examined (9+ to 14+) compared to αS alone postincubation (Figure 6b), whereas this trend was not consistent at lower charge states (4+ to 8+). Overall, the data indicate that C-PC prevents the conformational collapse of highly disordered αS monomers that precedes aggregation, thereby inhibiting fibril formation.

Understanding the mechanisms by which amyloid fibril formation can be inhibited offers fundamental insight into the protein misfolding and aggregation process and potential for the rational design of therapeutic agents to prevent amyloidogenic diseases. The cyanobacterium *Arthrospira (Spirulina) platensis* is mainly thought of as a source of nutraceuticals. However, this study demonstrates, using a range of biophysical and biochemical approaches, that a major component of this bacterium, C-PC, is an effective inhibitor of amyloid fibril formation.

The inhibition of αS and Aβ fibril formation by C-PC was shown to be significantly effective at extreme substoichiometric ratios (down to 200:1). This inhibition by C-PC is reminiscent of the chaperone-like activity of sHsps, in that they both effectively inhibit fibril formation of various aggregation-prone proteins at substoichiometric ratios in an ATP-independent manner.[32−35] Both sHsps and C-PC do not refold destabilized proteins to their native state (a process that requires other molecular chaperones in an ATP-dependent manner), but rather "hold" destabilized proteins to prevent them from further destabilization and subsequent aggregation. Other

DOI: 10.1021/acs.jnatprod.8b00610
J. Nat. Prod. 2019, 82, 66−73

proteins, other than sHsps, that act in an ATP-independent manner have also been shown to be effective inhibitors of protein aggregation, such as SerpinB2 against Aβ40,[36] in addition to small molecules such as the polyphenols curcumin and kaempferol, which effectively inhibit fibrillation of lysozyme[37] and (−)-epi-gallocatechine gallate, which has been shown to remodel preformed αS mature fibrils.[38] However, unlike the sHsps, the inhibitory action of C-PC is specific to aggregation-prone proteins that form amyloid fibrils, as our data demonstrate that C-PC is relatively ineffective in arresting amorphous aggregation.

The interactions responsible for preventing αS amyloid fibril formation by C-PC were examined by various techniques such as 2D NMR, native MS, IM-MS, and analytical-SEC. The lack of distinct chemical shift changes observed by 2D NMR, in addition to the absence of large complexes between αS and C-PC being observed via MS (which typically enhance electrostatic interactions between αS and C-PC if present[39,40]) and analytical-SEC, clearly demonstrates that the interactions responsible in inhibiting fibril formation are nonstable and likely to be a weak and/or transient. This finding is consistent with similar studies that demonstrate that the interaction between Aβ and sHsps (αB-crystallin) is also transient.[41] It is also possible that C-PC binds to αS through nonspecific associations with hydrophobic regions of αS that protrude from the cross-Aβ fibril core. The IM-MS data indicate αS undergoes a considerable conformational change toward more compact structures prior to fibril formation, consistent with a disorder to order transition with β-sheet formation prior to fibril formation as observed previously.[42] It is apparent, however, that in the presence of C-PC, the αS monomers consistently show CCS values (and in turn conformations) that lie between αS before and after incubation. It is therefore likely that binding of C-PC results in some structural rearrangement and stabilization of extended structures comparable in conformation to monomeric αS.

The combination of effective fibril inhibition at substoichiometric ratios, the absence of strong binding interactions with αS, and the observation that C-PC does not significantly dissociate preformed fibrils suggests that simple sequestration is not the mechanism responsible for the anti-amyloidogenic properties of C-PC. Furthermore, the absence of protein complexes and the lack of visible binding interactions with C-PC and αS also indicate that the interactions involved in fibril formation inhibition are nonstable but rather transient with soluble fibrillogenic proteins, which subtly alter the structure, dynamics, or equilibrium of αS fibrillation. Future studies should focus on further elucidating the nature and affinity of the interaction of C-PC with amyloidogenic proteins, providing additional information in our understanding of the mechanisms responsible in the formation and inhibition of amyloid fibrils that might aid in therapeutic development.

EXPERIMENTAL SECTION

Sample Preparation. A53TαS expression was carried out using an *Escherichia coli* BL21 (DE3) cell line containing the gene of human αS (UniProt accession number: P37840) with an A53T mutation inserted into a pRSETB vector (Invitrogen). Cells were grown in LB medium for nonlabeled αS or M9 minimal media with uniformly labeled [^{15}N] NH_4Cl (Sigma) for ^{15}N-labeled αS. Protein expression was induced with 1 mM isopropyl β-D-1-thiogalactopyranoside and purified as described previously.[43] Aβ40, Aβ42, and C-PC were purchased from Anaspec. Alcohol dehydrogenase (ADH) and catalase were acquired from Sigma-Aldrich. The concentrations of αS, ADH, and catalase were determined by using the extinction coefficients of 5120 M^{-1} cm^{-1} (280 nm), 41 170 M^{-1} cm^{-1} (280 nm), and 38 000 M^{-1} cm^{-1} (405 nm), respectively, on a Cary 5000 UV−visible NIR spectrophotometer (Varian). Aβ40/42 stocks (238 μM in 500 mM ammonium acetate) were pretreated with NaOH to ensure Aβ monomerization (i.e., prevent preoligomeric/fibril formation) prior to being used in the aggregation assays. All proteins solutions were stored at −80 °C before use.

Fibrillar and Amorphous Aggregation Assays. Fibril formation of αS (10 μM) or Aβ40/42 (10 μM) was monitored using a thioflavin-T fluorescence assay[21] over a period of 100 h at 37 °C. Assays were performed in 500 mM ammonium acetate (pH 7.4) in sealed 384-microwell plates and measured on a FLUOstar Optima plate reader (BMG Lab Technologies). The inhibition of fibril formation by C-PC was performed at a range of substoichiometric molar ratios of αS (2:1, 5:1, 10:1, 50:1, and 200:1) (αS:C-PC) and Aβ40/42 (5:1) (Aβ:C-PC). ThT fluorescence was monitored using a 440/490 nm excitation/emission filter set. The ability of C-PC to inhibit αS fibril formation was quantified by comparing the ThT fluorescence of αS in the presence of C-PC relative to αS alone (as a percentage) at the end-point of the aggregation assay (100 h), as previously described.[44]

The amorphous aggregation of ADH was monitored by the change in absorbance as a result of light scattering at 340 nm over a period of 2 h at 42 °C.[45] Aggregation of ADH (5 μM) was induced by the addition of 20 mM DTT and 2 mM EDTA (final concentration). The heat-induced aggregation of catalase (5 μM) was also measured by changes in absorbance over a period of 2 h at 55 °C.[44] The ability of C-PC to inhibit the amorphous aggregation of ADH and catalase was performed in the absence and presence of C-PC at a range of substoichiometric molar ratios (1:1, 2:1, and 5:1) (ADH/catalase:C-PC). All amorphous aggregation assays were performed in sealed 384-microwell plates and measured on a FLUOstar Optima plate reader (BMG Lab Technologies). All assays were performed in triplicate and reported as mean ± SEM.

TEM Imaging. The overall morphology of αS and Aβ fibrils was imaged by TEM, in which 5 μL aliquots from the end-point of the ThT aggregation assays were adsorbed onto carbon-coated electron microscopy grids (SPI Supplies) and negatively stained with 2% (w/v) uranyl acetate. Images were viewed using a Philip CM100 transmission electron microscope at a magnification of 34 000×.

2D NMR Spectroscopy. The interaction between αS and C-PC was examined by NMR spectroscopy, where ^{15}N-labeled αS (150 μM in 10 mM Na_2HPO_4, 100 mM NaCl, pH 7.4 in 10% D_2O) was analyzed in the absence and presence of C-PC (7.5 μM). Two-dimensional ^{1}H−^{15}N HSQC experiments were performed at 10 °C on a 600 MHz Unity Inova NMR spectrometer (Varian). The spectra were recorded using 128 complex points, 8 scans per increment, and a relaxation delay of 1.2 s. Processed HSQC spectra were analyzed using CcpNmr analysis software[46] in combination with previously reported assignments.[47,48]

Ion Mobility−Mass Spectrometry. IM-MS was performed on a Synapt G1 HDMS (Waters) with a nanoelectrospray source. αS (10 μM) and C-PC (2 μM) in 500 mM ammonium acetate (pH 7.0) were loaded onto platinum-coated borosilicate glass capillaries prepared in-house (Harvard Apparatus). Instrument parameters were optimized for maintaining noncovalent complexes and were typically as follows: capillary voltage, 1.8 kV; sample cone voltage, 60 V; source temperature, 25 °C; trap collision energy, 10 V; transfer collision energy, 20 V; trap gas, 2.77×10^{-2} mbar; backing pressure, 3.0 mbar. Typical IM cell instrument parameters: wave velocity, 300 m/s; IM cell pressure, 4.0×10^{-1} mbar. The arrival time distributions were recorded at three different wave heights (8, 8.5, and 9 V). Calculated collision cross-section (in Å^2) area values were determined by using serum amyloid precursor protein, myoglobin, cytochrome *c*, and ubiquitin as calibrants according to protocols reported elsewhere.[49]

Analytical Size-Exclusion Chromatography. The interaction between αS and C-PC was examined by analytical size-exclusion chromatography.[34] Samples (approximately 10 μM) from fibrillar aggregation assays were centrifuged at 15000*g* for 30 min at 4 °C to

DOI: 10.1021/acs.jnatprod.8b00610
J. Nat. Prod. 2019, 82, 66−73

remove aggregated proteins. The cleared supernatant was loaded onto Superdex 200 10/300 GL analytical-SEC (GE Healthcare), equilibrated in 500 mM NH_4OAc (pH 6.8), at a flow rate of 0.4 mL/min at room temperature. The size-exclusion column was calibrated using standards (Sigma-Aldrich) containing bovine thyroglobulin (670 kDa), bovine γ-globulin (158 kDa), chicken ovalbumin (44 kDa), and horse myoglobin (17 kDa).

■ ASSOCIATED CONTENT

Supporting Information

The Supporting Information is available free of charge on the ACS Publications website at DOI: 10.1021/acs.jnatprod.8b00610.

Figures of X-ray crystal structure of the C-PC dodecamer from *Spirulina platensis* and turbidity assay of αS in the presence of C-PC in ammonium acetate and phosphate buffer systems (PDF)

■ AUTHOR INFORMATION

Corresponding Author

*Tel: +61 8 8313 5497. Fax: +61 8 8313 4381. E-mail: tara.pukala@adelaide.edu.au.

ORCID

Tara L. Pukala: 0000-0001-7391-1436

Author Contributions

§Y. Liu and B. Jovcevski contributed equally to this work.

Notes

The authors declare no competing financial interest.

■ ACKNOWLEDGMENTS

We thank Dr. L. A. O'Donovan and Adelaide Microscopy (both University of Adelaide, Australia) for TEM technical assistance. We also thank Flinders Analytical (Flinders University, Australia) for access and support to IM-MS instrumentation. This research was supported in part by an Australian Research Council Discovery Project Grant (DP1093143 and DP170102033).

■ REFERENCES

(1) Chiti, F.; Dobson, C. M. *Annu. Rev. Biochem.* **2006**, *75* (1), 333−366.
(2) Inouye, H.; Fraser, P. E.; Kirschner, D. A. *Biophys. J.* **1993**, *64* (2), 502−519.
(3) Moreau, K. L.; King, J. A. *Trends Mol. Med.* **2012**, *18* (5), 273−282.
(4) Nie, Q.; Du, X. G.; Geng, M. Y. *Acta Pharmacol. Sin.* **2011**, *32* (5), 545−551.
(5) Sloan, L. A.; Fillmore, M. C.; Churcher, I. *Curr. Opin. Drug Discovery Dev.* **2009**, *12* (5), 666−681.
(6) Liu, T.; Bitan, G. *ChemMedChem* **2012**, *7* (3), 359−374.
(7) Young, L. M.; Ashcroft, A. E.; Radford, S. E. *Curr. Opin. Chem. Biol.* **2017**, *39*, 90−99.
(8) Hartl, F. U.; Bracher, A.; Hayer-Hartl, M. *Nature* **2011**, *475* (7356), 324−332.
(9) Mayer, M. P. *Mol. Cell* **2010**, *39* (3), 321−331.
(10) Saibil, H. *Nat. Rev. Mol. Cell Biol.* **2013**, *14* (10), 630−642.
(11) Saibil, H. *Nat. Rev. Mol. Cell Biol.* **2013**, *14* (10), 630−642.
(12) Welch, W. J. *Semin. Cell Dev. Biol.* **2004**, *15* (1), 31−38.
(13) McHaourab, H. S.; Godar, J. A.; Stewart, P. L. *Biochemistry* **2009**, *48* (18), 3828−3837.
(14) Yébenes, H.; Mesa, P.; Muñoz, I. G.; Montoya, G.; Valpuesta, J. M. *Trends Biochem. Sci.* **2011**, *36* (8), 424−432.
(15) Vadiraja, B. B.; Gaikwad, N. W.; Madyastha, K. M. *Biochem. Biophys. Res. Commun.* **1998**, *249* (2), 428−431.
(16) Romay, C.; Gonzalez, R.; Ledon, N.; Remirez, D.; Rimbau, V. *Curr. Protein Pept. Sci.* **2003**, *4* (3), 207−216.
(17) Chen, T.; Wong, Y.-S. *J. Agric. Food Chem.* **2008**, *56* (12), 4352−4358.
(18) Kao, O. H.; Berns, D. S.; Town, W. R. *Biochem. J.* **1973**, *131* (1), 39−50.
(19) Kao, O. H.; Edwards, M. R.; Berns, D. S. *Biochem. J.* **1975**, *147* (1), 63−70.
(20) Li, X.; Ma, L.; Zheng, W.; Chen, T. *Biomaterials* **2014**, *35* (30), 8596−604.
(21) Nilsson, M. R. *Methods* **2004**, *34* (1), 151−160.
(22) Dedmon, M. M.; Christodoulou, J.; Wilson, M. R.; Dobson, C. M. *J. Biol. Chem.* **2005**, *280* (15), 14733−14740.
(23) Waudby, C. A.; Knowles, T. P. J.; Devlin, G. L.; Skepper, J. N.; Ecroyd, H.; Carver, J. A.; Welland, M. E.; Christodoulou, J.; Dobson, C. M.; Meehan, S. *Biophys. J.* **2010**, *98* (5), 843−851.
(24) Rekas, A.; Adda, C. G.; Andrew Aquilina, J.; Barnham, K. J.; Sunde, M.; Galatis, D.; Williamson, N. A.; Masters, C. L.; Anders, R. F.; Robinson, C. V.; Cappai, R.; Carver, J. A. *J. Mol. Biol.* **2004**, *340* (5), 1167−1183.
(25) Heck, A. J. R. *Nat. Methods* **2008**, *5* (11), 927−933.
(26) Hernandez, H.; Robinson, C. V. *Nat. Protoc.* **2007**, *2* (3), 715−726.
(27) Ruotolo, B. T.; Benesch, J. L.; Sandercock, A. M.; Hyung, S. J.; Robinson, C. V. *Nat. Protoc.* **2008**, *3* (7), 1139−1152.
(28) Clemmer, D. E. Clemmer collision cross-section database http://www.indiana.edu/~clemmer/, accessed 19/02/2018.
(29) Bernstein, S. L.; Liu, D.; Wyttenbach, T.; Bowers, M. T.; Lee, J. C.; Gray, H. B.; Winkler, J. R. *J. Am. Soc. Mass Spectrom.* **2004**, *15* (10), 1435−1443.
(30) Liu, Y.; Ho, L. H.; Carver, J. A.; Pukala, T. L. *Aust. J. Chem.* **2011**, *64* (1), 36−40.
(31) Uversky, V. N.; Li, J.; Fink, A. L. *J. Biol. Chem.* **2001**, *276* (14), 10737−10744.
(32) Cox, D.; Selig, E.; Griffin, M. D.; Carver, J. A.; Ecroyd, H. *J. Biol. Chem.* **2016**, *291* (43), 22618−22629.
(33) Jovcevski, B.; Kelly, M. A.; Rote, A. P.; Berg, T.; Gastall, H. Y.; Benesch, J. L.; Aquilina, J. A.; Ecroyd, H. *Chem. Biol.* **2015**, *22* (2), 186−195.
(34) Kulig, M.; Ecroyd, H. *Biochem. J.* **2012**, *448* (3), 343−352.
(35) Mainz, A.; Peschek, J.; Stavropoulou, M.; Back, K. C.; Bardiaux, B.; Asami, S.; Prade, E.; Peters, C.; Weinkauf, S.; Buchner, J.; Reif, B. *Nat. Struct. Mol. Biol.* **2015**, *22* (11), 898−905.
(36) Lee, J. A.; Yerbury, J. J.; Farrawell, N.; Shearer, R. F.; Constantinescu, P.; Hatters, D. M.; Schroder, W. A.; Suhrbier, A.; Wilson, M. R.; Saunders, D. N.; Ranson, M. *PLoS One* **2015**, *10* (6), e0130136.
(37) Borana, M. S.; Mishra, P.; Pissurlenkar, R. R.; Hosur, R. V.; Ahmad, B. *Biochim. Biophys. Acta, Proteins Proteomics* **2014**, *1844* (3), 670−680.
(38) Bieschke, J.; Russ, J.; Friedrich, R. P.; Ehrnhoefer, D. E.; Wobst, H.; Neugebauer, K.; Wanker, E. E. *Proc. Natl. Acad. Sci. U. S. A.* **2010**, *107* (17), 7710−7715.
(39) Daniel, J.; Friess, S.; Rajagopalan, S.; Wendt, S.; Zenobi, R. *Int. J. Mass Spectrom.* **2002**, *216* (1), 1−27.
(40) Yin, S.; Xie, Y.; Loo, J. A. *J. Am. Soc. Mass Spectrom.* **2008**, *19* (8), 1199−1208.
(41) Das, P.; Kang, S. G.; Temple, S.; Belfort, G. *PLoS One* **2014**, *9* (11), e113041.
(42) Conway, K. A.; Harper, J. D.; Lansbury, P. T. *Nat. Med.* **1998**, *4* (11), 1318−1320.
(43) Volles, M. J.; Lansbury, P. T., Jr *J. Mol. Biol.* **2007**, *366* (5), 1510−1522.
(44) Ecroyd, H.; Carver, J. A. *FEBS J.* **2008**, *275* (5), 935−947.
(45) Mymrikov, E. V.; Daake, M.; Richter, B.; Haslbeck, M.; Buchner, J. *J. Biol. Chem.* **2017**, *292* (2), 672−684.
(46) Vranken, W. F.; Boucher, W.; Stevens, T. J.; Fogh, R. H.; Pajon, A.; Llinas, M.; Ulrich, E. L.; Markley, J. L.; Ionides, J.; Laue, E. D. *Proteins: Struct., Funct., Genet.* **2005**, *59* (4), 687−696.

DOI: 10.1021/acs.jnatprod.8b00610
J. Nat. Prod. 2019, 82, 66−73

(47) Eliezer, D.; Kutluay, E.; Bussell, R., Jr.; Browne, G. *J. Mol. Biol.* **2001**, *307* (4), 1061−1073.
(48) Kang, L.; Janowska, M. K.; Moriarty, G. M.; Baum, J. *PLoS One* **2013**, *8* (9), e75018.
(49) Ruotolo, B. T.; Benesch, J. L.; Sandercock, A. M.; Hyung, S. J.; Robinson, C. V. *Nat. Protoc.* **2008**, *3* (7), 1139−1152.

DOI: 10.1021/acs.jnatprod.8b00610
J. Nat. Prod. 2019, 82, 66−73